Defence Research and
Development Canada

Recherche et développement
pour la défense Canada

DEFENCE **R&D** DÉFENSE

A basic Fourier transform pair for slant range-Doppler modeling of moving scatterers for SAR applications
Theory

R. Sabry

Defence R&D Canada – Ottawa

Canada

A basic Fourier transform pair for slant range-Doppler modeling of moving scatterers for SAR applications

Theory

R. Sabry
Defence R&D Canada - Ottawa

Defence R&D Canada – Ottawa

Technical Memorandum
DRDC Ottawa TM 2007-289
November 2007

Principal Author

Original signed by Ramin Sabry

Ramin Sabry

Defence Scientist

Approved by

Original signed by Gary Geling

Gary Geling

Section Head, Radar Applications and Space Technology

Approved for release by

Original signed by Pierre Lavoie

Pierre Lavoie

Chief Scientist Defence R&D Canada - Ottawa

Abstract

Considering the exploitation needs associated with the Synthetic Aperture Radar (SAR) applications involving moving and non-stationary targets, a fundamental spectral domain model for moving point and distribution of scatterers is presented. The approach is accurate as the spherical phase front is rigorously treated throughout the Doppler analysis. Due to the analytic nature of the model in range-Doppler plain, large squint-angle operations (e.g., SpotSAR) can be characterized. Furthermore, motion characteristics can be extracted in the sub-aperture level to better reflect the general motion (e.g., non-uniform). As a result, enhanced adaptivity can be achieved to improve the imagery and other target-signature measured products. The range-Doppler model can serve as a tool for polarimetric and multi-channel analysis.

Résumé

Compte tenu des besoins d'exploitation associés aux applications SAR (radar à synthèse d'ouverture) utilisées avec des cibles mobiles et non stationnaires, nous présentons ici un modèle fondamental dans le domaine spectral, applicable aux points mobiles et à la distribution de diffuseurs. Cette approche est exacte, car le front de phase sphérique est traité rigoureusement tout au long de l'analyse Doppler. Étant donné la nature analytique du modèle dans le plan distance-Doppler, de grandes opérations à angle de strabisme (p. ex. SpotSAR) peuvent être caractérisées. En outre, les caractéristiques de mouvement peuvent être extraites au niveau sous-ouverture pour mieux représenter le mouvement général (p. ex. non uniforme). Par conséquent, l'adaptivité peut être accrue pour améliorer l'imagerie et d'autres produits mesurés de signature de cibles. Le modèle distance-Doppler peut servir d'outil pour l'analyse polarimétrique et multi-canal.

This page intentionally left blank.

Executive summary

A basic Fourier transform pair for slant range-Doppler modeling of moving scatterers for SAR applications: theory

Ramin Sabry; DRDC Ottawa TM 2007-289; Defence R&D Canada – Ottawa; November 2007.

Background: Synthetic aperture radar (SAR) provides means for fine-resolution detection and imagery by virtue of the synthetically created coherent gain. Conventional SAR technologies use certain established techniques to characterize and exploit the coherent phase and create imagery. All mainstream techniques, however, use phase simplification strategies (e.g., plane-wave approximation in a tomographic paradigm) to approximate the spherical phase. Such widely used approximations become less adequate and more problematic when exploiting the moving targets imagery for motion modeling, modifications (e.g., focusing) and target recognition. An analytic range-Doppler model to characterize canonical moving point scatterers is developed here. The approach is accurate as the spherical phase front variations and Doppler effects due to the target motion are directly modeled in slant range-Doppler domain without the need for range and azimuth de-coupling.

Results: The system response or Green's function for imaging a collection or distribution of moving scatterers is derived and established by taking advantage of the developed coherent range-Doppler model. Application of the range-Doppler system model in conjunction with the measured data and/or image yields target velocity information. On this basis, a velocity extraction algorithm is also developed to characterize the motion of the scatterer or target. The range-Doppler model can also be used to define the motion corrected matched-filter transfer function for re-focusing the SAR image.

Significance: Certain classes of applications would largely benefit from the accuracy of the developed technique where methods based on the conventional phase expansions (e.g., series, Fresnel) would not be effective. Squint mode of operation (larger squint angles, in particular) can be modeled more correctly using the developed approach. Also, wider synthetic aperture operations, i.e., large integration time, can be handled. The coherent nature of the model offers accurate motion extraction through effective utilization of the phase information. Means for sub-aperture analysis is provided which enables characterization of the motion variations within the synthetic aperture acquisition time.

Sommaire

A basic Fourier transform pair for slant range-Doppler modeling of moving scatterers for SAR applications: theory

Ramin Sabry; DRDC Ottawa TM 2007-289; R & D pour la défense Canada – Ottawa; Novembre 2007.

Introduction : Le radar à synthèse d'ouverture (RSO) permet la détection et l'imagerie à haute résolution au moyen d'un gain cohérent créé par synthèse. Les technologies RSO classiques utilisent certaines techniques établies pour caractériser et exploiter la phase cohérente et produire des images. Toutes les techniques courantes font toutefois appel à des stratégies de simplification de phase (p. ex. approximation d'onde plane dans un paradigme tomographique) pour s'approcher de la phase sphérique. Ces approximations largement utilisées sont moins satisfaisantes et plus problématiques lorsqu'on exploite l'imagerie de cibles mobiles pour la modélisation du mouvement, des modifications (p. ex. mise au point) et la reconnaissance de cibles. Nous élaborons ici un modèle Doppler analytique en fonction de la distance pour caractériser des diffuseurs ponctuels mobiles canoniques. Cette approche est précise, car les variations du front de phase sphérique et les effets Doppler dus au mouvement des cibles sont directement modélisés dans le domaine Doppler à distance oblique sans nécessiter de découplage en distance et en azimut.

Résultats : Le modèle Doppler élaboré à distance cohérente permet de déterminer la réponse du système ou la fonction de Green pour l'imagerie du regroupement ou de la distribution de diffuseurs mobiles. L'application du modèle du système Doppler en fonction de la distance et l'utilisation des images et/ou données mesurées fournissent de l'information sur la vitesse des cibles. De même, un algorithme d'extraction de la vitesse est établi pour caractériser le mouvement d'un diffuseur ou d'une cible. Le modèle Doppler en fonction de la distance peut aussi servir à définir la fonction de transfert à filtrage adapté et correction selon le mouvement pour refaire la mise au point d'une image de RSO.

Portée : Certaines classes d'applications profiteraient largement de la précision de la technique élaborée lorsque les méthodes fondées sur des expansions de phase ordinaires (p. ex. en série et de Fresnel) s'avéreraient inefficaces. La méthode établie permet de modéliser plus correctement le mode de fonctionnement à strabisme (plus grands angles de strabisme, en particulier). Elle se prête aussi au traitement des ouvertures synthétiques plus larges, c.-à-d. aux longues durées d'intégration. La nature cohérente du modèle procure une extraction de mouvement précise par l'utilisation efficace de l'information de phase. Des moyens d'analyse de sous-ouverture peuvent caractériser les variations de mouvement durant l'acquisition d'ouverture synthétique.

Table of contents

List of figures

List of tables

This page intentionally left blank.

1 Introduction

Synthetic aperture radar (SAR) provides a means for fine-resolution detection and imagery by the virtue of a synthetically created long antenna as the result of antenna or sensor motion [1]-[2]. Different modes of SAR operation, e.g., single channel, polarimetric, enjoy growing interest due to unique properties of a SAR based operation for remote sensing. In addition to the high resolution property and the ability to operate in non-cooperative conditions, advantageous SAR characteristics can be best represented by the three conservation principles [1]; conservation of energy, confusion and coordinates. The first two principles highlight the radiometric characteristics where the latter represents the spatial performance of the SAR system. These attractive SAR properties, however, are accompanied by their own sets of challenges. Considering the coherent nature of SAR operation, proper treatment of phase is highly important. Judicious phase modeling and characterization becomes even more critical when the scattering centers are not stationary. In such scenarios, care should be taken in approximation or decomposition of the spherical phase front.

Current SAR technologies (e.g., airborne and space borne SAR, PolSAR, ISAR) use established techniques to characterize and exploit the coherent phase and create imagery. In range-Doppler processing, the range dimension of the image is established through the resolution of fast time delays. The azimuth dimension is established by the Doppler gradient of the radar signal phase function across the scene. All mainstream techniques, however, use phase simplification strategies (e.g., plane-wave approximation in a tomographic paradigm) to approximate the spherical phase. These approximations, which can yield good results, depending on the applied technique and imaging application, are needed to develop a practical imaging system. However, the same argument is not valid for the advanced exploitation of SAR imagery. Such widely used approximations become less adequate and more problematic when exploiting the moving targets imagery for motion modeling, modifications (e.g., focusing) and target recognition.

Despite the existence of significant theoretical work and applied techniques in the literature [3]-[9], it is not easy to find a robust algorithm or methodology to resolve the exploitation and focusing difficulties associated with real moving targets (e.g., non-uniform motion, moving multi-scatterers, ships). This is, undoubtedly, a great challenge due to many contributing factors and is not intended to be entirely resolved here. Rather, the intent is to address the challenge by investigating the impact of accurate phase modeling. The present approach is based on the analytic modeling of point and distributed moving targets (i.e., Green's function formalism) in the range-Doppler domain through aperture and sub-aperture. The principle of stationary phase (PSP) [10] is employed that is accurate for typical large time-bandwidth SAR signals. As such, the need for phase decoupling (range-azimuth) is removed. In fact, the majority of advanced techniques (e.g., [6]-[9]) aim to account for the range curvature and compensate or correct for range migration, residuals and high order effects resulting from the spherical phase decomposition. On this basis, the approach here can provide better accuracy for high squint angle and long aperture modes of operation. Moreover, due to Fourier transform and PSP properties, the conventional plane wave approximation is avoided. This shift-varying property improves the range-Doppler accuracy of the moving scattering centers.

Range-Doppler frequency domain analysis is suitable for multi-channel and polarimetric investigations as the need for time domain interpolation is removed. This interpolation to co-register non-simultaneously acquired channels (e.g., cross polarimetric channels) is used for coherent target classification analysis and often is the source of error resulting in incorrect interpretations and exploitations. For instance, a stationary target may be assumed moving due to de-correlation of its polarimetric scattering vectors.

An analytical framework and methodology is established here with pointers to the type of applications that benefit from this approach. At the present, the experimental scope is limited to comparing the simulated canonical moving scatterer range-Doppler characteristics. This core comparison would indicate the relative precision achieved for the ultimate product exploitation and focusing.

2 Theory

Assume a moving scatterer with large time-bandwidth radar return signal product. Figure 1 depicts the associated SAR configuration and moving scatterer or target geometry. The SAR sensor and moving target positions are denoted by P_s and P_m, respectively. One can mathematically represent the echoed SAR signal by:

$$S(x,r) = A(x)\,P(r - R(x))\exp(-j2k\,R(x))\exp(-j\alpha(r - R(x))^2)$$

(1)

Where,

$A(x)$: Azimuth antenna pattern,

$P(r)$: Range pulse envelope,

α : Pulse fm rate determining the bandwidth and resolution,

$k = \dfrac{2\pi}{\lambda}$: Propagation wavenumber, λ being the operating wavenumber,

and x, r denote azimuth and slant range directions respectively. One should note that x, r are not mathematically orthogonal and should be treated so.
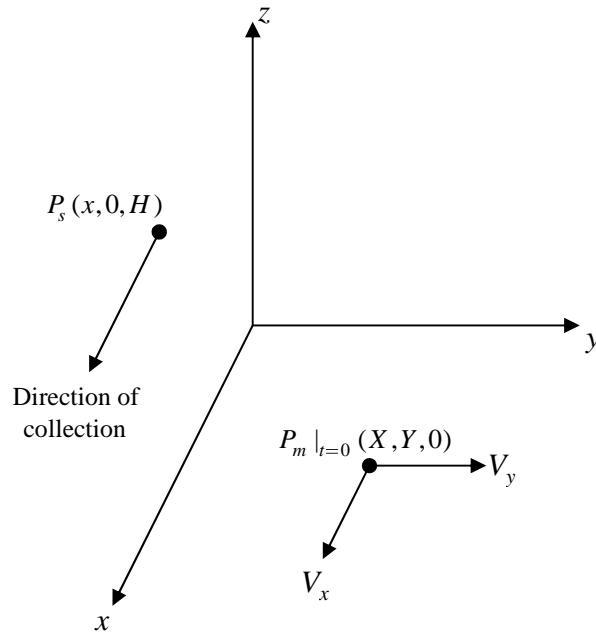

Figure 1. Moving Target SAR Imaging Geometry

Represent the range history function for a scatterer undertaking uniform motion with a generic form:

$$R(x) = \sqrt{R_0{}^2 + m^2 (x - x_0)^2} \qquad\qquad (2)$$

where R_0 is the equivalent slant range of the closest approach (orthogonal to azimuth), the range-Doppler slope m is a dimensionless factor representing the normalized (by stationary target rate) Doppler rate, and x_0 represents the equivalent or shifted scatterer azimuth position (Doppler center). For a stationary target ($m = 1$), R_0 and x_0 become the conventional slant range of the closest approach and scattering center azimuth position. The range history function in (2) can model any type of target motion. As will be addressed later in this section and analyzed in the next section, general motion is characterized by introducing time-dependent m, R_0 and x_0, i.e., $m(x)$, $R_0(x)$ and $x_0(x)$, in the range history equation (2). For the range-Doppler variations in this section, however, a constant velocity motion is assumed, i.e., time-independent m, R_0 and x_0. Employing the principle of stationary phase (PSP), the range-azimuth frequency (i.e., Doppler) transform of the waveform (1) is calculated. Due to non-orthogonality of the range and azimuth pairs (i.e., range curvature), conventional direct azimuth transformation neglecting the curvature is not analytically correct. Such approximations limit and/or suppress insights into the exploitation/imaging process and may result in considerable error. To resolve this difficulty and maintain the analytic consistency, a two step approach is undertaken [5]. As the first step (that can be viewed as a two-step process itself), a two dimensional correlated Fourier transform is performed. This is done by performing the range Fourier transformation followed by an azimuth Fourier transformation when the azimuth dependence of the range curvature is taken into considerations. The second step would be to perform an inverse range Fourier transformation to the range-Doppler frequency domain. The described process can be summarized by the schematic depicted in Figure 2.

To apply PSP for Fourier transformation, one must solve for the stationary point of the total phase associated with the Fourier integrand, i.e.,

$$\delta \Psi_{total} = 0 \qquad\qquad (3)$$

and use the result to compute the Fourier integral in the vicinity of the stationary point. Employing PSP in the slant range (r) dimension, i.e., $\dfrac{\partial \Psi^{x,r}(x,r)}{\partial r} = 0$, one gets (according to (1)):

$$\tilde{S}(x,\omega_r) = C_0 \, A(x) \, P(-\frac{\omega_r}{2\alpha}) \exp(\,j\,\frac{\omega_r^2}{4\alpha}) \exp(-\,j(2k+\omega_r)\,R(x)) \qquad (4)$$

where ω_r (rad/m) is the range space frequency.

Re-employing PSP in the azimuth (x) dimension, i.e., $\dfrac{\partial \Psi^{x,\omega_r}(x,\omega_r)}{\partial x} = 0$, one must solve the stationary point equation (according to (4)):

$$\frac{d\,R(x)}{dx}\bigg|_{x=x_s} = -\frac{\omega_x}{(2k+\omega_r)} \qquad (5)$$

where ω_x (rad/m) is the azimuth space frequency. Using (2) one obtains:

$$\tilde{S}(\omega_x,\omega_r) = C_1 \, A(x_0 - \frac{R_0\omega_x}{2km^2\,[(1+\frac{\omega_r}{2k})^2 - \frac{\omega_x^2}{4k^2m^2}]^{\frac{1}{2}}}).$$

$$P(-\frac{\omega_r}{2\alpha})\exp(\,j\,\frac{\omega_r^2}{4\alpha}). \qquad (6)$$

$$\exp(-\,j2kR_0\,[\,(1+\frac{\omega_r}{2k})^2 - \frac{\omega_x^2}{4k^2m^2}]^{\frac{1}{2}})\exp(-\,j\omega_x x_0)$$

In order to derive the range-Doppler characteristics of the SAR signal, an inverse range Fourier transform is applied. This would require solution of the stationary point equation $\dfrac{\partial \Psi^{\omega_x,\omega_r}(\omega_x,\omega_r)}{\partial \omega_r} = 0$, which takes the form (according to (6)):

$$r + \frac{\omega_r}{2\alpha} - \frac{R_0\,(1+\frac{\omega_r}{2k})}{[(1+\frac{\omega_r}{2k})^2 - \frac{\omega_x^2}{4k^2m^2}]^{\frac{1}{2}}} = 0 \qquad (7)$$

Expanding the term associated with the square root denominator in (7) using:

$$(1+\delta)^{-\frac{1}{2}} = 1 - \frac{1}{2}\delta + \frac{3}{8}\delta^2 + \mathbf{O}(\delta^3) \tag{8}$$

and assuming a typical bandwidth (linewidth):

$$\frac{\frac{\omega_r}{k} + \frac{\omega_r^2}{4k^2}}{1 - \frac{\omega_x^2}{4k^2m^2}} \ll 1 \tag{9}$$

one can rewrite (7), for the phase to the order of $\mathbf{O}(\omega_r^3)$ as:

$$\frac{\omega_r}{2\alpha'} + r - R_\Omega(\omega_x) = 0 \tag{10}$$

where

$$\frac{1}{\alpha'} = \frac{1}{\alpha} + \frac{R_0\,\omega_x^2}{4k^3m^2(1 - \frac{\omega_x^2}{4k^2m^2})^{\frac{3}{2}}} \tag{11}$$

$$R_\Omega(\omega_x) = \frac{R_0}{(1 - \frac{\omega_x^2}{4k^2m^2})^{\frac{1}{2}}} \tag{12}$$

Applying the solution of (10) for the stationary point ω_r and using (6), one derives the range-Doppler description of the SAR signal as:

$$\tilde{S}(\omega_x, r) = C_2 \, A(x_0 - \frac{R_0 \omega_x}{2km^2[(1 - \frac{\alpha'}{k}(r - R_\Omega(\omega_x)))^2 - \frac{\omega_x^2}{4k^2 m^2}]^{\frac{1}{2}}}) \cdot$$

$$P(\frac{\alpha'}{\alpha}(r - R_\Omega(\omega_x))) \exp(j \frac{\alpha'^2}{\alpha}(r - R_\Omega(\omega_x))^2) \cdot \qquad (13)$$

$$\exp(-j2kR_0[(1 - \frac{\alpha'}{k}(r - R_\Omega(\omega_x)))^2 - \frac{\omega_x^2}{4k^2 m^2}]^{\frac{1}{2}}) \exp(-j\omega_x x_0)$$

C_0, C_1, C_2 in (4),(6) and (13) are complex constants.

The above equations suggest that one could ultimately define a range-Doppler domain Green's system function for multi-scatterers as:

$$\tilde{G}(r, \omega_x, X, Y, m) = \tilde{S}(\omega_x, r) \qquad (14)$$

where X, Y determine the initial position of the moving scatterer. One can express the target equations of general motion as:

$$X(t) = X + V_x(t) t \qquad (15)$$

$$Y(t) = Y + V_y(t) t \qquad (16)$$

where $V_x(t)$ and $V_y(t)$ are the generalized velocity functions. Considering the sensor or radar platform altitude H and velocity v_a, and setting $t = \dfrac{x}{v_a}$ one can write the general range history function of a moving scatterer as:

$$R^2(x) = (x - X(t))^2 + Y(t)^2 + H^2$$
$$= (x - X - \gamma_x(x)x)^2 + (Y + \gamma_y(x)x)^2 + H^2 \qquad (17)$$

where

$$\gamma_x(x) = \frac{V_x\left(\dfrac{x}{v_a}\right)}{v_a} \tag{18}$$

$$\gamma_y(x) = \frac{V_y\left(\dfrac{x}{v_a}\right)}{v_a} \tag{19}$$

Expanding (17) and comparing with (2), for general motion one obtains:

$$m(x) = \sqrt{\gamma_y(x)^2 + (1 - \gamma_x(x))^2} \tag{20}$$

$$x_0(x) = \frac{(1 - \gamma_x(x))X - \gamma_y(x)Y}{\gamma_y(x)^2 + (1 - \gamma_x(x))^2} \tag{21}$$

$$R_0(x)^2 = \frac{\left[\gamma_y(x)^2 + (1 - \gamma_x(x))^2\right]H^2 + \left[(1 - \gamma_x(x)) + \gamma_y(x)\dfrac{X}{Y}\right]^2 Y^2}{\left[\gamma_y(x)^2 + (1 - \gamma_x(x))^2\right]} \tag{22}$$

For a constant velocity or uniform motion:

$$\gamma_x(x) = \gamma_x = \frac{V_x}{v_a} \tag{23}$$

$$\gamma_y(x) = \gamma_y = \frac{V_y}{v_a} \tag{24}$$

and $m(x)$, $x_0(x)$, $R_0(x)$ become constant m, x_0, R_0 in (2) defined by (20)-(22) with $\gamma_{x,y}(x) \rightarrow \gamma_{x,y}$.

Using (13), the system Green's function for a uniformly moving rigid body of scatterers can be written as:

$$\tilde{G}(r,\omega_x,X,Y,\gamma_x,\gamma_y) = A(x_0 - \frac{R_0\omega_x}{2km^2[(1-\frac{\alpha'}{k}(r-R_\Omega(\omega_x)))^2 - \frac{\omega_x^2}{4k^2m^2}]^{\frac{1}{2}}}) \cdot$$

$$P(\frac{\alpha'}{\alpha}(r-R_\Omega(\omega_x)))\exp(j\frac{\alpha'^2}{\alpha}(r-R_\Omega(\omega_x))^2) \cdot$$

$$\exp(-j2kR_0[(1-\frac{\alpha'}{k}(r-R_\Omega(\omega_x)))^2 - \frac{\omega_x^2}{4k^2m^2}]^{\frac{1}{2}})\exp(-j\omega_x x_0)$$

(25)

where $\alpha', R_\Omega(\omega_x)$ are defined by (11)-(12) and constants m, x_0, R_0 are given by (20)-(22) ($\gamma_{x,y}(x) \to \gamma_{x,y}$). Thus, the overall range-Doppler characteristic of a moving cluster or distribution is described by:

$$\tilde{S}_D(\omega_x,r,\gamma_x,\gamma_y) = \iint\limits_{area} f_D(X,Y,\gamma_x,\gamma_y)\tilde{G}(r,\omega_x,X,Y,\gamma_x,\gamma_y)\,dX\,dY \qquad (26)$$

where $f_D(X,Y,\gamma_x,\gamma_y)$ represents the moving scatterers' stationary scattering distribution function. Dependence of the above distribution function on γ_x and γ_y accounts for the variations in scattering or RCS fading due to the movement. If these effects are negligible, the velocity dependence may be dropped, i.e., $f_D(X,Y)$, and the motion effects will be included in the range-Doppler Green's function.
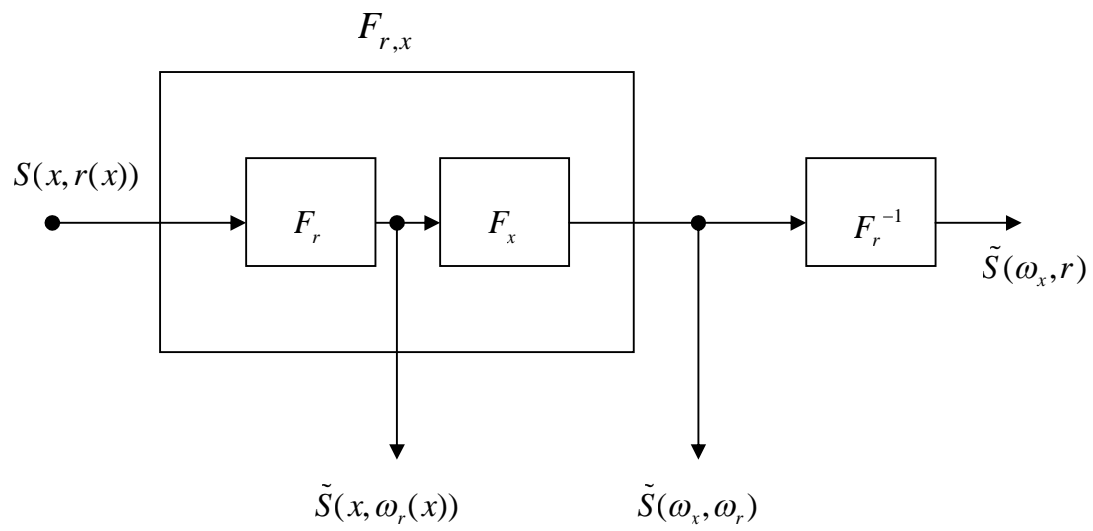
Figure 2. Multi-step Fourier Transform Process

3   Non-Uniform Motion Correction

The analytic range-Doppler frequency model developed is accurate for constant velocity target motion assumptions. The method can be generalized to non-uniform or varying velocity motions by assuming the conservation of large time-bandwidth product (TBP). This is done by introducing a method for correcting stationary point of the variational phase.

The mathematics of the addressed correction technique is more involved due to the nonlinear motion. Here, however, certain assumptions are made that are judicious and can provide a feasible yet accurate methodology. The stationary point equation is given by (5) that is valid for any type of motion. This stationary point location is dependent on the non-uniform motion due to the associated range function variations, i.e., left-hand-side of equation (5). As addressed in the definition of (2), for non-uniform motion the range function is given by:

$$R(x) = \sqrt{R_0(x)^2 + m(x)^2 (x - x_0(x))^2} \tag{27}$$

where $m(x)$, $x_0(x)$, $R_0(x)$ are described by (20)-(22).

The exact solution of (5) for the corrected stationary point can be written in a general form:

$$x_s = X_s(\omega_x, \omega_r) \tag{28}$$

As pointed out, this solution is involved. However, if the velocity variations are not severe, one may assume $m(x), x_0(x), R_0(x)$ are slow varying functions. More specifically if:

$$\frac{\frac{d}{dx}[R_0(x)]^2}{2m(x)^2(x - x_0(x))} + (x - x_0(x))\frac{d}{dx}\ln(m(x)) - \frac{d}{dx}x_0(x) \ll 1 \tag{29}$$

upon invoking the slow varying assumption and solving for the stationary points (4)-(5), one can derive the corrected Fourier transform as:

$$\tilde{S}_c(\omega_x,\omega_r) = C_1 \, A(x_0(X_s(\omega_x,\omega_r))) - \frac{R_0(X_s(\omega_x,\omega_r))\omega_x}{2km^2(X_s(\omega_x,\omega_r))[(1+\frac{\omega_r}{2k})^2 - \frac{\omega_x^2}{4k^2 m^2(X_s(\omega_x,\omega_r))}]^{\frac{1}{2}}}) \cdot$$

$$P(-\frac{\omega_r}{2\alpha})\exp(j\frac{\omega_r^2}{4\alpha}) \cdot$$

$$\exp(-j2kR_0(X_s(\omega_x,\omega_r))).[\,(1+\frac{\omega_r}{2k})^2 - \frac{\omega_x^2}{4k^2 m^2(X_s(\omega_x,\omega_r))}]^{\frac{1}{2}}).$$

$$\exp(-j\omega_x x_0(X_s(\omega_x,\omega_r)))$$

$$(30)$$

To derive the range-Doppler transform for the non-uniform motion, an inverse range Fourier transform on (30) is to be applied that involves the stationary point solution for ω_r, similar to one described in (7). This solution, however, is more complicated due to dependence of R_0, m and x_0 functions on ω_r. In order to develop a feasible and yet accurate solution, a two step approach is undertaken for mathematical manipulations. As the first step, the azimuth stationary point solution (28) to the general stationary point equation (5) is approximated through (or in the vicinity of) a zeroth order solution of (7) for ω_r. In the next step, this approximated stationary point is used to define the overall phase function in (30) to solve for the higher order solution of (7) for ω_r. Providing that the exact solution of the stationary phase for ω_r is variational about the described zeroth order solution, the associated higher order solution would be accurate reflecting the general motion due to the variational property [11]-[12].

To obtain the zeroth order solution, it is assumed (further to the slow-varying assumption) functions $R_0(\omega_x,\omega_r)$, $m(\omega_x,\omega_r)$ and $x_0(\omega_x,\omega_r)$ are variational about a stationary ω_r point. A judicious choice for this stationary point is the one determined by the average motion (i.e., velocity) within the aperture or sub-aperture of interest. Characteristics of this point are defined by:

$$\overline{m} = \sqrt{\overline{\gamma}_y^2 + (1-\overline{\gamma}_x)^2} \qquad (31)$$

$$\overline{R}_0^2 = \frac{\left[\overline{\gamma}_y^2 + (1-\overline{\gamma}_x)^2\right]H^2 + \left[(1-\overline{\gamma}_x)+\overline{\gamma}_y\frac{X}{Y}\right]^2 Y^2}{\left[\overline{\gamma}_y^2 + (1-\overline{\gamma}_x)^2\right]} \qquad (32)$$

$$\bar{x}_0 = \frac{(1-\bar{\gamma}_x)X - \bar{\gamma}_y Y}{\bar{\gamma}_y{}^2 + (1-\bar{\gamma}_x)^2} \tag{33}$$

where $\bar{\gamma}_x$ and $\bar{\gamma}_y$ are the average target velocities (relative) within the aperture of interest. Accordingly, similar to the procedure performed in (7)-(10), one can solve for the zeroth order stationary point $\bar{\omega}_r{}^{(s)}$ using:

$$\frac{\bar{\omega}_r{}^{(s)}}{2\bar{\alpha}'} + r - \frac{\bar{R}_0}{(1 - \dfrac{\omega_x{}^2}{4k^2\bar{m}^2})^{\frac{1}{2}}} = 0 \tag{34}$$

where:

$$\frac{1}{\bar{\alpha}'} = \frac{1}{\alpha} + \frac{\bar{R}_0 \omega_x{}^2}{4k^3\bar{m}^2(1 - \dfrac{\omega_x{}^2}{4k^2\bar{m}^2})^{\frac{3}{2}}} \tag{35}$$

Thus, the corrected stationary azimuth point (28) can be approximated by:

$$x_s = X_s(\omega_x, -2\bar{\alpha}'(r - \frac{\bar{R}_0}{(1 - \dfrac{\omega_x{}^2}{4k^2\bar{m}^2})^{\frac{1}{2}}})) \tag{36}$$

where $X_s(\omega_x, \omega_r)$ is the solution of (5) for the general target motion.

As addressed before, the higher order or more accurate solution, namely $\omega_r{}^{(s)}$, for the stationary phase can be found by using (36) to define the overall phase function in (30). Doing so, the range frequency stationary point satisfies the equation:

$$\frac{\omega_r^{(s)}}{2\tilde{\alpha}'} + r - \tilde{R}_\Omega(\omega_x) = 0 \tag{37}$$

where,

$$\frac{1}{\tilde{\alpha}'} = \frac{1}{\alpha} + \frac{R_0(x_s)\omega_x^2}{4k^3 m^2(x_s)(1 - \frac{\omega_x^2}{4k^2 m^2(x_s)})^{\frac{3}{2}}} \tag{38}$$

$$\tilde{R}_\Omega(\omega_x) = \frac{R_0(x_s)}{(1 - \frac{\omega_x^2}{4k^2 m^2(x_s)})^{\frac{1}{2}}} \tag{39}$$

Applying the stationary point solution (37) to perform the inverse range Fourier transform, one finds:

$$\tilde{S}_c(\omega_x, r) = C\, A(x_0(x_s) - \frac{R_0(x_s)\omega_x}{2km^2(x_s)[(1 - \frac{\tilde{\alpha}'}{k}(r - \tilde{R}_\Omega(\omega_x)))^2 - \frac{\omega_x^2}{4k^2 m^2(x_s)}]^{\frac{1}{2}}}) \cdot$$

$$P(\frac{\tilde{\alpha}'}{\alpha}(r - \tilde{R}_\Omega(\omega_x)))\exp(j\frac{\tilde{\alpha}'^2}{\alpha}(r - \tilde{R}_\Omega(\omega_x))^2) \cdot$$

$$\exp(-j2kR_0(x_s)[(1 - \frac{\tilde{\alpha}'}{k}(r - \tilde{R}_\Omega(\omega_x)))^2 - \frac{\omega_x^2}{4k^2 m^2(x_s)}]^{\frac{1}{2}})\exp(-j\omega_x x_0(x_s))$$

$$\tag{40}$$

Equation (40) provides a relatively rigorous yet analytically feasible means to model non-uniform target motion in the range-Doppler domain. For a uniform motion, (40) reduces to (13). The stationary point (azimuth) solution in (5) appears to be the problematic part for the non-uniform motion. In most cases, however, a solution can be found through analytic derivations and proper approximations. The applied approximations yield accurate results within the validity of the variational and slow-varying assumptions. These assumptions become even more judicious for sub-aperture analysis. For piecewise linear (i.e., uniform motion), the solution approaches the one

in (13) within the associated sub-aperture, hence providing an accurate model for sub-aperture analysis.

4   Range-Doppler Simulations

The effects of target or scatterer motion on the SAR image can be studied by the aid of described range-Doppler model. In doing so, motion characteristics may be investigated through the whole aperture or at the sub-aperture level. The latter is particularly desired when characterizing non-uniform or piecewise uniform target motions. In practice, the measured moving point target(s) range-Doppler response will be compared against the simulated model data to extract motion information and/or remove the associated effects from the SAR image, i.e., focusing. Range-Doppler characteristics of point targets with uniform and non-uniform motion are simulated and presented. Target motion parameters and SAR imaging system specifications are assumed to be similar to those of a typical airborne SAR scenario for possible further validations. Accordingly, it is assumed that the flight altitude $H = 6$ km and the incident angle $\theta_{inc} = 45°$.

In case of an uniform motion, the point target travels at a constant ground speed $V_x = 0.1 v_a$ and $V_y = 0.1 v_a$. The SAR platform or vehicle velocity v_a, is typically about 360 km/h for airborne SAR, hence, the overall ground speed of the moving target $V_g = 0.14 v_a$ is about 50 km/h. For non-uniform motion, the target moves with a similar initial speed $V_x = V_y = 0.1 v_a$ and accelerates by 5 m/s^2 at each direction. Thus, the overall ground acceleration reads as $a = 7.1$ m/s^2. For non-uniform motion, the analytic range-Doppler model is generalized to accommodate time varying velocity by correcting the point of stationary phase. Relatively accurate Doppler distribution can be obtained depending on the validity of phase variational assumption that is good for typical SAR signals. A narrow range pulse envelope is assumed for current simulations.

Figure 3 depicts the non-uniform motion effects on the range-azimuth history of a moving scatterer. As is seen, the already changed-shape and shifted range history of the target due to the uniform motion is further shape changed and shifted by introducing acceleration, i.e., non-uniform motion. Thus, the target image will be further smeared and shifted. An interesting observation, however, is the target image shift that is partially compensated by the acceleration. Associated range-Doppler (instantaneous) characteristics of the described movers are included in Figure 4. It is evident the non-uniform mover experiences more rapid and wider Doppler variations. Hence, application of a model based on the uniform motion assumption within the entire aperture can not be effective. Also, it is seen that the non-linear motion effects are more pronounced at the higher Doppler frequencies. Figure 5 illustrates a comprehensive comparison amongst the range-Doppler characteristics derived through present analytical approach, instantaneous using the exact range history, and instantaneous using the Fresnel approximated range history for a point target with non-uniform motion. In figures 4-5, the range-Doppler coordinate system (in Doppler direction) is centered at the zero-Doppler of the exact range-Doppler characteristic of the uniformly moving target. As seen, the analytic range-Doppler history is computed applying two models. One is based on the exact motion model for

generalized velocity functions $V_x(t)$ and $V_y(t)$ described by (15)-(16) and labeled as Instantaneous. The other is based on the same equation of motion but with velocities defined by the instantaneous derivatives of motion, i.e., $V_{xder}(t) = \dfrac{dX(t)}{dt}$ and $V_{yder}(t) = \dfrac{dY(t)}{dt}$, and labeled as derivative. A number of important observations are made through the inspection of Figure 5. Instantaneous Doppler variations resemble those found from the analytic approach using the motion derivatives. This is somewhat expected as instantaneous Doppler is also defined by the range function derivatives that involve motion derivatives. Results from a more rigorous analytic Doppler characterization (i.e., Inst.), however, differ from those of the described two. The outlined difference (although not very significant) underscores the fact that the instant Doppler description may not properly and accurately represent the true target Doppler distribution for non-linear motion. It is also evident that Fresnel phase approximation introduces considerable difference in terms of range-Doppler relations for moving point scatterer compared to the other techniques.

Inspection of the range relation (2) and system Green's function (25)-(26), along with the range-Doppler simulations of point scatterers reveals that point scatterers belonging to a moving cluster or target do not theoretically experience the same Doppler shift that results in shift and smearing in the image plane. Depending on the severity of this nonlinear effect that is related to a number of factors, e.g., size, resolution, image of a composite target may be further distorted and difficult to focus using conventional methods based on the point target assumption. If so, system Green's function formalism similar to (25)-(26) can be applied.
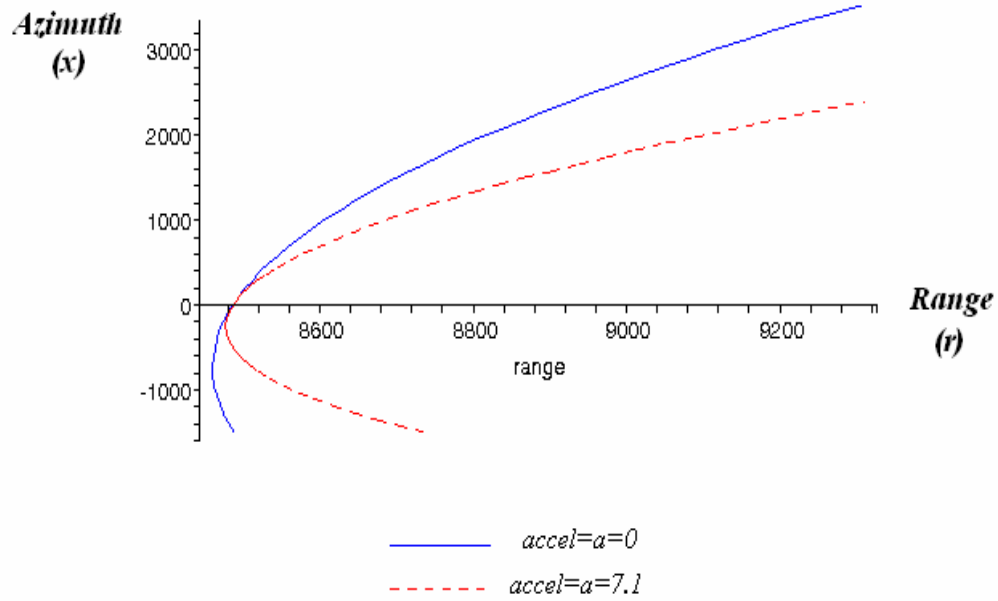
Figure 3. Slant Range-Azimuth History of Point Moving Target $(\gamma_x = 0.1, \gamma_y = 0.1)$
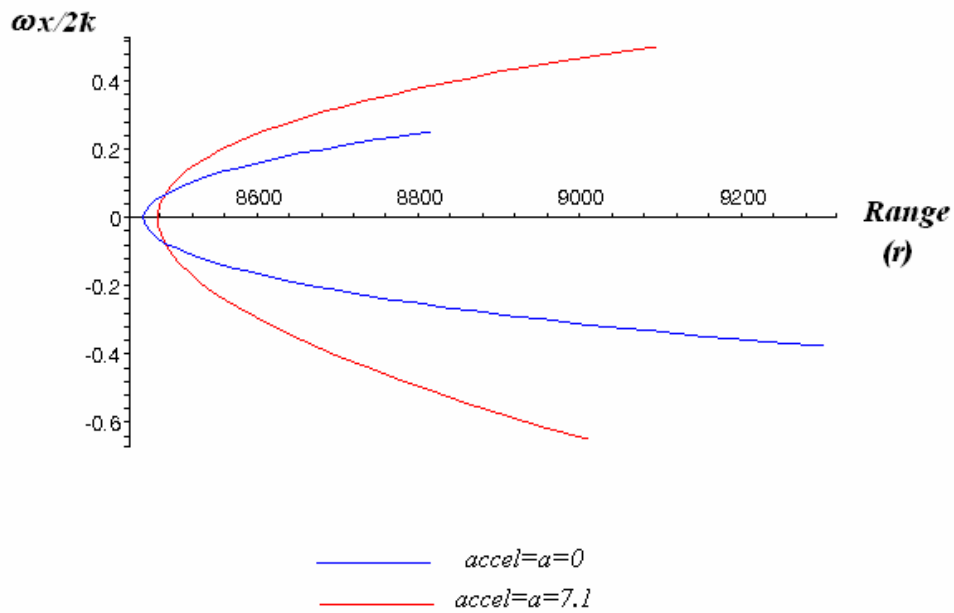

Figure 4. Instantaneous Slant Range-Doppler History of Point Moving Target
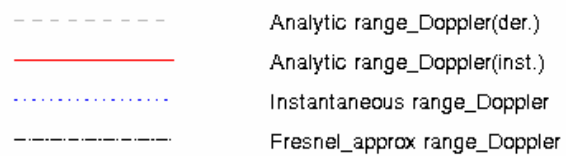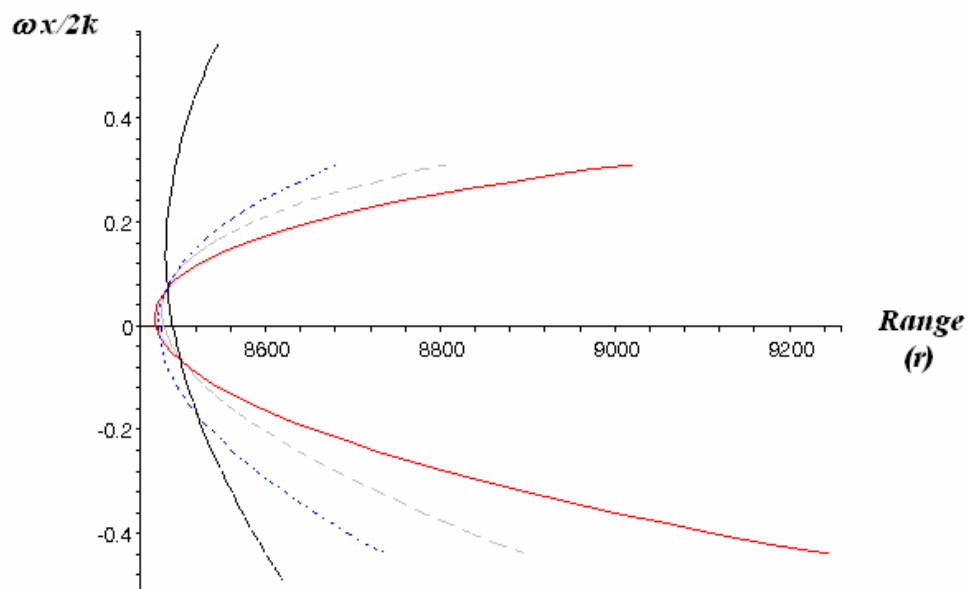$(\gamma_x = 0.1, \gamma_y = 0.1)$

Figure 5. Slant Range-Doppler History of Point Moving Target $(\gamma_x = 0.1, \gamma_y = 0.1, accel = a = 7.1)$ *: Comparison*

5   Velocity Extraction

One characteristic application of the range-Doppler model of moving scatterers is the velocity evaluation. Such velocity information and motion characteristics are used for advanced detection, focusing imagery and related target identification/recognition applications.

Technically, one can apply the developed model or Green's system function (25) to the range-Doppler history of a uniformly moving scatterer and extract the velocity information. For a group or cluster of moving scatterers, however, one (in theory) would need to solve the system integral equation (26) to derive the motion parameters. Uniform (i.e., constant velocity) motion is a good assumption for a variety of practical applications and targets (e.g., land targets). The model can also be applied for non-uniform motion at the sub-aperture level where velocity variations are negligible and motion is piecewise linear.

Inspection of (25) indicates that to characterize the motion of a persistent point scatterer on the target of interest, the associated trajectory in the range-Doppler domain must be tracked. This trajectory is given by:

$$r - R_{\Omega}(\omega_x) = 0 \tag{41}$$

Accordingly, the moving scatterer path in the range-Doppler plane is characterized by:

$$r = \frac{R_0}{(1 - \frac{\omega_x^2}{4k^2 m^2})^{\frac{1}{2}}} \tag{42}$$

Using (20)-(24), relation (42) may be written as:

$$r = \frac{\left(m^2 H^2 + Y^2 B^2\right)^{\frac{1}{2}}}{\left(m^2 - \xi^2\right)^{\frac{1}{2}}} \tag{43}$$

where

$$m^2 = \gamma_y^2 + (1 - \gamma_x)^2 \tag{44}$$

$$B = (1 - \gamma_x) + \gamma_y \frac{X}{Y} \qquad (45)$$

and $\xi = \dfrac{\omega_x}{2k}$ is the normalized Doppler frequency.

According to the above, the problem of moving scatterer tracking and velocity extraction would effectively transform to the optimal velocity (γ_x, γ_y) derivation for the respective range-Doppler history function. A least-square based technique is applied to compute the optimal velocity quantities from the range-Doppler history. However, instead of performing the optimization in terms of the relative velocity parameters (γ_x, γ_y), the error target function is minimized with respect to functions (44)-(45):

$$m = f_1(\gamma_x, \gamma_y) \qquad (46)$$

$$B = f_2(\gamma_x, \gamma_y) \qquad (47)$$

This can be shown to provide a more effective optimization.

Define the target function:

$$y = F(f_1(\gamma_x, \gamma_y), f_2(\gamma_x, \gamma_y), \xi) = \frac{\left(f_1^2(\gamma_x, \gamma_y) H^2 + Y^2 f_2^2(\gamma_x, \gamma_y) \right)^{\frac{1}{2}}}{\left(f_1^2(\gamma_x, \gamma_y) - \xi^2 \right)^{\frac{1}{2}}} \qquad (48)$$

Accordingly, the least-square optimization scheme is governed by the equation:

$$\frac{\partial}{\partial f_j} \left(\sum_{i=1..N} \left(y_i - F(f_1(\gamma_x, \gamma_y), f_2(\gamma_x, \gamma_y), \xi_i) \right)^2 \right) = 0, \qquad j = 1, 2 \qquad (49)$$

with "i" and "N" denoting the sample index number and total number of samples within the aperture or subaperture of interest.

As addressed, the choice of $f_1(\gamma_x, \gamma_y), f_2(\gamma_x, \gamma_y)$ yields analytic solution to (49) for the relative velocities $\bar{\gamma}_x, \bar{\gamma}_y$. Analytic derivations and solutions are included in Annex A.

In order to evaluate the efficiency of the model and the velocity extraction algorithm, one should apply the algorithm to the range-Doppler history of a moving scatterer with known motion. To do this, the range-Doppler characteristics of a point scatterer moving with constant velocity are simulated and used for velocity extraction applying the described procedure. These derivations and velocity estimations are performed for two cases of uniform motion, i.e., $\gamma_x = \gamma_y = 0.1$ and $\gamma_x = 0.17, \gamma_y = 0.23$. These motion parameters are chosen to somewhat emulate two typical and diverse cases of motion and operation.

The range-Doppler history simulations for the above two cases in the range-azimuth and range-Doppler frequency domains are depicted in Figures 6-9. The motion parameters used in simulations and respective computed velocities are included in Tables 1, 2. As seen, a higher incident angle $\theta_{inc} = 53.13°$ is chosen that is more typical for scenarios including ground moving targets. Moreover, to make it more general, a non-broadside moving target (i.e., non-zero Doppler at the initial state $t = 0$) is considered. The slant range-azimuth history of this non-broadside point target is presented in Figure 6 for a better understanding of the non-zero Doppler (i.e., squint) imaging of moving targets.
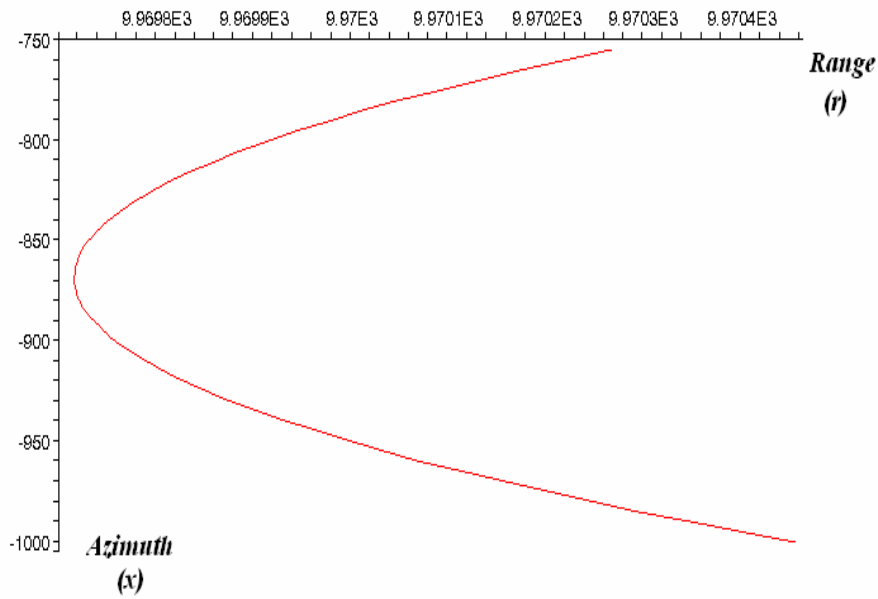
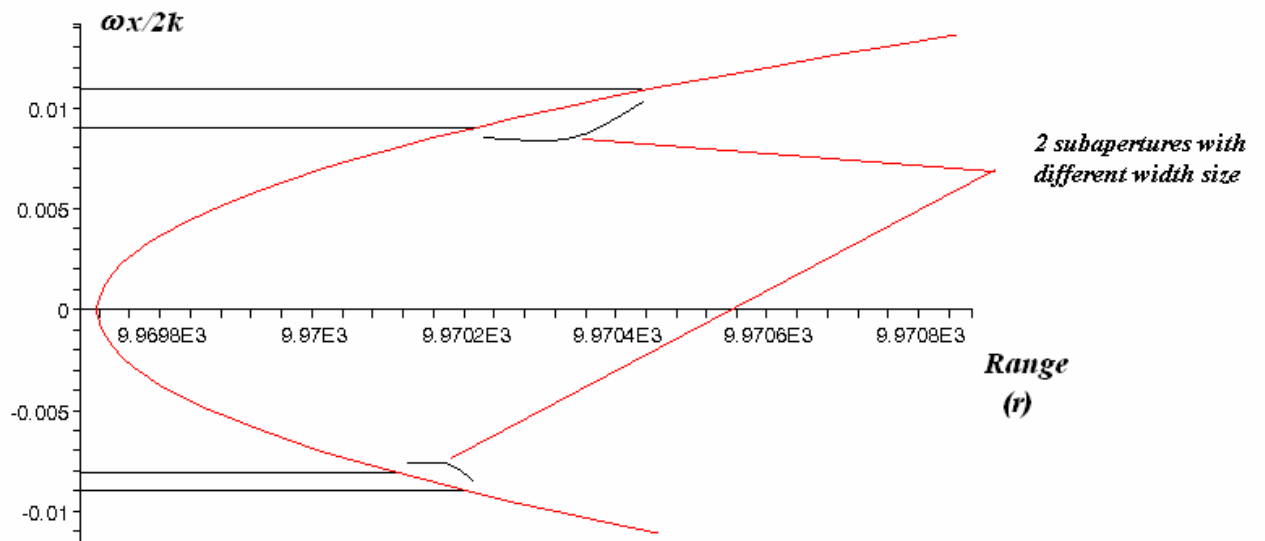*Figure 6. Slant Range-Azimuth History of Point Moving Target* $(\gamma_x = 0.1, \gamma_y = 0.1, X = 100m)$

Figure 7. Instantaneous Slant Range-Doppler History of Point Moving Target
$(\gamma_x = 0.1, \gamma_y = 0.1, X = 100m)$

Table 1 includes computed results for velocity extraction using the simulated range-Doppler history of a mover with motion parameters $\gamma_x = \gamma_y = 0.1$ (Figures 6-7) in 10 different subapertures within the total aperture. The sizes of subapertures (Doppler width) are chosen to be equal while utilizing the whole available aperture, i.e., the available aperture divided into 10 equal segments. As can be seen, computed velocity parameters are in good agreement (less than 1% error) with the parameters used in simulations or equivalent truthing.

Motion Parameters Used in the Range History Simulation						Extracted/Calculated Motion Parameters				
Subaperture #	γ_x	γ_y	$X_{(m)}$	$Y_{(m)}$	$H_{(m)}$	N	m^2	B^2	$\overline{\gamma}_x$	$\overline{\gamma}_y$
1	0.1	0.1	100	8000	6000	10	.820415	.812662	.099772	.100024
2	0.1	0.1	100	8000	6000	10	.820198	.812448	.099891	.100011
3	0.1	0.1	100	8000	6000	10	.819896	.812149	.100056	.099993
4	0.1	0.1	100	8000	6000	10	.819494	.811750	.100277	.099969
5	0.1	0.1	100	8000	6000	10	.819905	.812158	.100051	.099994
6	0.1	0.1	100	8000	6000	10	.820510	.812757	.099719	.100031
7	0.1	0.1	100	8000	6000	10	.819724	.811978	.100151	.099983
8	0.1	0.1	100	8000	6000	10	.820883	.813126	.099515	.100053
9	0.1	0.1	100	8000	6000	10	.820090	.812340	.099950	.100005
10	0.1	0.1	100	8000	6000	10	.820122	.812373	.099932	.100007

Table 1. Simulated and Computed Motion Parameters for Point Moving Target
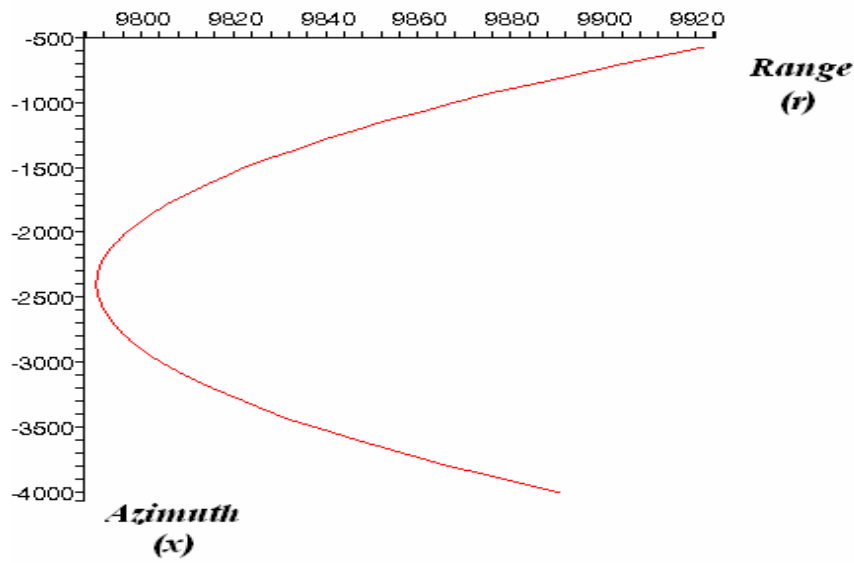$(\gamma_x = 0.1, \gamma_y = 0.1, X = 100m)$

Figure 8. Slant Range-Azimuth History of Point Moving Target
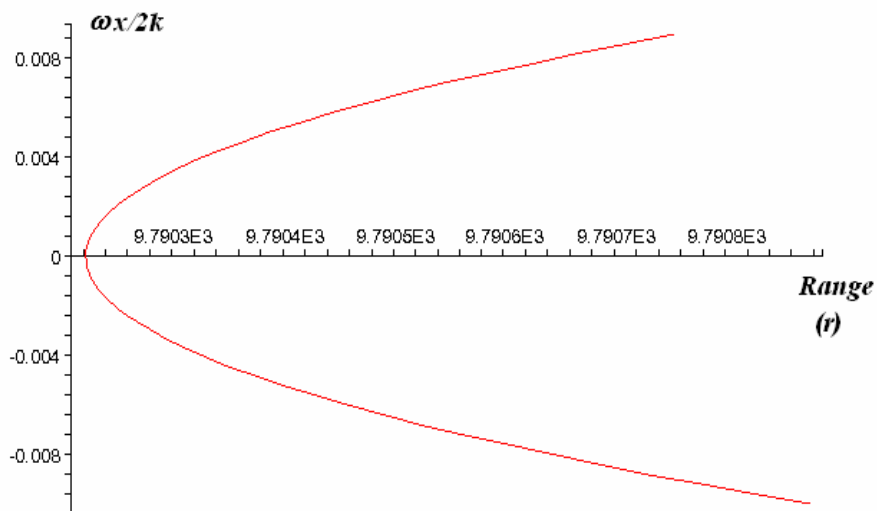$(\gamma_x = 0.17, \gamma_y = 0.23, X = 100m)$

Figure 9. Instantaneous Slant Range-Doppler History of Point Moving Target $(\gamma_x = 0.17, \gamma_y = 0.23, X = 100m)$

Computed velocity parameters for a mover with motion parameters $\gamma_x = 0.17, \gamma_y = 0.23$ are provided in Table 2. Simulated range-azimuth/range-Doppler characteristics are given by Figures 8-9. Again, a good agreement with the mover's true motion parameters (simulated) is evident (less than 1% error). To examine the applicability of the present algorithm to various parts of the available Doppler spectrum (synthetic aperture) or subapertures, an additional subaperture #11 is considered for velocity extraction. This subaperture is arbitrarily chosen within the total aperture and has a different width size and center location from other subapertures.

Motion Parameters Used in the Range History Simulation						Extracted/Calculated Motion Parameters				
Subaperture #	γ_x	γ_y	$X_{(m)}$	$Y_{(m)}$	$H_{(m)}$	N	m^2	B^2	$\overline{\gamma}_x$	$\overline{\gamma}_y$
1	0.17	0.23	100	8000	6000	10	.741641	.693531	.170089	.229975
2	0.17	0.23	100	8000	6000	10	.741784	.693666	.170008	.229997
3	0.17	0.23	100	8000	6000	10	.741789	.693671	.170005	.229998
4	0.17	0.23	100	8000	6000	10	.741682	.693570	.170065	.229981
5	0.17	0.23	100	8000	6000	10	.742027	.693893	.169872	.230035
6	0.17	0.23	100	8000	6000	10	.742027	.693893	.169872	.230035
7	0.17	0.23	100	8000	6000	10	.741606	.693499	.170108	.229969
8	0.17	0.23	100	8000	6000	10	.741514	.693414	.170159	.229955
9	0.17	0.23	100	8000	6000	10	.741784	.693666	.170008	.229997
10	0.17	0.23	100	8000	6000	10	.741725	.693611	.170041	.229988
11	0.17	0.23	100	8000	6000	20	.742177	.694033	.169789	.230058

Table 2. Simulated and Computed Motion Parameters for Point Moving Target
$(\gamma_x = 0.17, \gamma_y = 0.23, X = 100m)$

6   Conclusions

The appropriate choice of the backscattering signal model is highly important for effective SAR data/image exploitations. The need for such a robust analytic modeling is more critical for operations involving moving targets. There exist conventional models with their own set of advantages and shortcomings depending on the type of exploitation applications. Considering the coherent principle and nature of SAR imaging and associated products, accuracy of the SAR signal model is provided through accurate characterization of the basic spherical phase. On this basis, an analytic range-Doppler model to characterize canonical moving point scatterers is developed. This coherent model is used to establish the system response or Green's function for imaging a collection or distribution of moving scatterers. The approach is accurate as the spherical phase front variations and Doppler effects due to the target motion are directly modeled in slant range-Doppler domain without the need for range and azimuth de-coupling. The slant range-azimuth Green's function formalism is mathematically robust as it utilizes the signal space data, and reflects the electromagnetic physics of scattering as the exact Green's function for a point source is defined in slant range. Also, the range band-limited property is incorporated in the formulation of target Doppler distribution.

The developed model enjoys certain attractive characteristics. Accurate modeling of range variations and its azimuth dependence provides better prediction of range-Doppler behaviour of the moving scatterer. Higher squint angle and wider synthetic aperture modes of operation would benefit from such accuracy, where, conventional phase expansions (e.g., series, Fresnel) would not be suitable. Furthermore, the target dependent shift-varying property (conventionally ignored through the plane wave approximation process) is captured. Application of the range-Doppler model in conjunction with the measured data or image yields target velocity information. It can also be used to define the matched-filter transfer function for image re-focusing. The means for sub-aperture analysis is provided which enables characterization of motion variations within the synthetic aperture acquisition time. Results shown indicate accurate derivation of velocity parameters for a given mover using various subapertures of range-Doppler data (in terms of center location and width size). The model is generalized to treat nonlinear target motion. This generalized model is relatively involved but is accurate and practical to study and treat the localized effects. Moreover, adopting a sub-aperture approach and assuming piecewise linear motion, the uniform motion range-Doppler model can be locally applied.

The key contribution of the present work may be viewed as providing a canonical picture of motion effects on the range-Doppler frequency characteristics. One important observation is that the scatterer motion is more consistently analyzed and modeled in slant range-Doppler domain. Accordingly, the model validation and required experimentation are more meaningful in such domain.

Actual experimentation based on real imagery will be presented in an ensuing communication due to unavailability of such results at the time of submission. Furthermore, considering the importance of experimental verifications a complete paper ought to be dedicated to the experimentations, validations and interpretations. There are no standard measures/metrics for

focusing evaluation that are solely based on the final focused image. More objective assessments incorporating the focused target response signal characteristics or at the intermediate stage (e.g., range-Doppler) is needed for proper validations. Such measured validations become more important where the imagery products are used for classification and recognition purposes.

References

[1] F.M. Henderson, A.J. Lewis, Eds., *Principles & Applications of Imaging Radars,* Third Edition, Volume 2, John Wiley & Sons, NY, 1998.

[2] C. Elachi, Spaceborne Radar Remote Sensing: Applications and Techniques, IEEE Press, New York, 1988.

[3] Soumekh, M., Synthetic Aperture Radar Signal Processing, NY: Wiley, 1999.

[4] R. Sabry and P. W. Vachon, "A spectral domain approach to modeling of EM scattering for Synthetic Aperture Radar target recognition," Waves in Random and Complex Media (formerly Waves in Random Media, Institute of Physics, UK), Volume 15, Number 3, August 2005, pp. 375-394.

[5] R. K. Raney, "A New and Fundamental Fourier Transform Pair," Proceedings of the International Geoscience and Remote Sensing Symposium, IGARSS'92, Clear Lake, TX, May 1992, pp. 106-107.

[6] R. K. Raney, H. Runge, R. Bamler, I. Cumming, and F. Wong, "Precision SAR Processing Using Chirp Scaling," IEEE Trans. Geosci. Remote Sens., Volume 32, Number 4, Jul. 1994, pp. 786–799.

[7] J. Mittermayer, A. Moreira, and O. Loffeld, "Spotlight SAR Data ProcessingUsing the Frequency Scaling Algorithm," IEEE Trans. Geosci. Remote Sens., Volume 37, Number 5, Sep. 1999, pp. 2198–2214.

[8] A. Papoulis, The Fourier Integral and Its Applications. New York: McGraw-Hill, 1962.

[9] J. L. Walker, "Range-Doppler imaging of rotating objects," IEEE Trans. Aerosp. Electron. Syst., Volume AES-16, Number 1, Jan. 1980, pp. 23–52.

[10]   M. Born and E. Wolf, Principles of Optics, Pergamon Press, MacMillan, NY, 1959, Appendix III.

[11]   Harrington, R.F., Field Computation by Moment Methods, Krieger Publishing Company, Inc., Malabar, Florida, 1982.

[12]   Jones, D.S., "A Critique of the Variational Method in Scattering Problems," IRE Trans., Vol. AP-4, pp. 297-301, 1956.

This page intentionally left blank.

Annex A   Velocity Analytic Description

Solution to the range-Doppler error target function optimization (49) for moving scatterer velocity components can be derived through considerable amount of analytic manipulations (to the order of $\dfrac{3}{8}\dfrac{\xi^4}{f_1^{\,5}}, i.e., \mathbf{O}\left(\dfrac{3}{8}\dfrac{\xi^4}{m^5}\right)$), as:

$$m^2 = f_1^{\,2}(\overline{\gamma}_x, \overline{\gamma}_y) = \frac{1}{2}\frac{\sum_N y_i \sum_N \xi_i^{\,4} - \sum_N \xi_i^{\,2} \sum_N y_i \xi_i^{\,2}}{N \sum_N y_i \xi_i^{\,2} - \sum_N y_i \sum_N \xi_i^{\,2}} \tag{A1}$$

$$B^2 = f_2^{\,2}(\overline{\gamma}_x, \overline{\gamma}_y) = \frac{M^2 - m^2 H^2}{Y^2} \tag{A2}$$

where

$$M = \frac{m^5 \sum_N y_i + \dfrac{1}{2} m^3 \sum_N y_i \xi_i^{\,2}}{N m^4 + m^2 \sum_N \xi_i^{\,2} + \dfrac{1}{4} \sum_N \xi_i^{\,4}} \tag{A3}$$

Velocity components $\overline{\gamma}_x, \overline{\gamma}_y$ can be found by solving the system of equations (44)-(45) using the results for m, B obtained from (A1)-(A3).

List of symbols/abbreviations/acronyms/initialisms

DND	Department of National Defence
DRDC	Defence Research & Development Canada
DRDKIM	Director Research and Development Knowledge and Information Management
ISAR	Inverse Synthetic Aperture Radar
PSP	Principle of Stationary Phase
PolSAR	Polarimetric Synthetic Aperture Radar
R&D	Research & Development
SAR	Synthetic Aperture Radar
TBP	Time Bandwidth Product

Distribution list

Document No.: DRDC Ottawa TM 2007-289

LIST PART 1: Internal Distribution by Centre

1	G. Geling
1	D. Schlingmeier
1	P. Vachon
1	R. Sabry
2	Library

6	TOTAL LIST PART 1

LIST PART 2: External Distribution by DRDKIM

3	Library and Archives Canada
1	ADM (S&T)
1	CFJIC (Attn. Capt N.W. Scanlan)
1	DRDKIM

6	TOTAL LIST PART 2

12   TOTAL COPIES REQUIRED

SECURITY CLASSIFICATION OF FORM
(highest classification of Title, Abstract, Keywords)

DOCUMENT CONTROL DATA
(Security classification of title, body of abstract and indexing annotation must be entered when the overall document is classified)

1. ORIGINATOR (the name and address of the organization preparing the document. Organizations for whom the document was prepared, e.g. Establishment sponsoring a contractor's report, or tasking agency, are entered in section 8.) Defence R&D Canada - Ottawa 3701 Carling Avenue Ottawa, ON, K1A 0Z4	2. SECURITY CLASSIFICATION (overall security classification of the document, including special warning terms if applicable) UNCLASSIFIED

3. TITLE (the complete document title as indicated on the title page. Its classification should be indicated by the appropriate abbreviation (S,C or U) in parentheses after the title.)

A Basic Fourier Transform Pair for Slant Range-Doppler Modeling of Moving Scatterers for SAR Applications: Theory

4. AUTHORS (Last name, first name, middle initial)

Sabry, R.

5. DATE OF PUBLICATION (month and year of publication of document) November 2007	6a. NO. OF PAGES (total containing information. Include Annexes, Appendices, etc.) 42	6b. NO. OF REFS (total cited in document) 12

7. DESCRIPTIVE NOTES (the category of the document, e.g. technical report, technical note or memorandum. If appropriate, enter the type of report, e.g. interim, progress, summary, annual or final. Give the inclusive dates when a specific reporting period is covered.)

Technical Memorandum

8. SPONSORING ACTIVITY (the name of the department project office or laboratory sponsoring the research and development. Include the address.)

DRDC OTTAWA
3701 Carling Avenue
Ottawa, ON, K1A 0Z4

9a. PROJECT OR GRANT NO. (if appropriate, the applicable research and development project or grant number under which the document was written. Please specify whether project or grant) 15ec05	9b. CONTRACT NO. (if appropriate, the applicable number under which the document was written)
10a. ORIGINATOR'S DOCUMENT NUMBER (the official document number by which the document is identified by the originating activity. This number must be unique to this document.) DRDC Ottawa TM 2007-289	10b. OTHER DOCUMENT NOS. (Any other numbers which may be assigned this document either by the originator or by the sponsor)

11. DOCUMENT AVAILABILITY (any limitations on further dissemination of the document, other than those imposed by security classification)

(x) Unlimited distribution
( ) Distribution limited to defence departments and defence contractors; further distribution only as approved
( ) Distribution limited to defence departments and Canadian defence contractors; further distribution only as approved
( ) Distribution limited to government departments and agencies; further distribution only as approved
( ) Distribution limited to defence departments; further distribution only as approved
( ) Other (please specify):

12. DOCUMENT ANNOUNCEMENT (any limitation to the bibliographic announcement of this document. This will normally correspond to the Document Availability (11). However, where further distribution (beyond the audience specified in 11) is possible, a wider announcement audience may be selected.)

Unliminited

SECURITY CLASSIFICATION OF FORM

DCD03   2/06/87

13. ABSTRACT (a brief and factual summary of the document. It may also appear elsewhere in the body of the document itself. It is highly desirable that the abstract of classified documents be unclassified. Each paragraph of the abstract shall begin with an indication of the security classification of the information in the paragraph (unless the document itself is unclassified) represented as (S), (C), or (U). It is not necessary to include here abstracts in both official languages unless the text is bilingual).

(U) Considering the exploitation needs associated with the Synthetic Aperture Radar (SAR) applications involving moving and non-stationary targets, a fundamental spectral domain model for moving point and distribution of scatterers is presented. The approach is accurate as the spherical phase front is rigorously treated throughout the Doppler analysis. Due to the analytic nature of the model in range-Doppler plain, large squint-angle operations (e.g., SpotSAR) can be characterized. Furthermore, motion characteristics can be extracted in the sub-aperture level to better reflect the general motion (e.g., non-uniform). As a result, enhanced adaptivity can be achieved to improve the imagery and other target-signature measured products. The range-Doppler model can serve as a tool for polarimetric and multi-channel analysis.

14. KEYWORDS, DESCRIPTORS or IDENTIFIERS (technically meaningful terms or short phrases that characterize a document and could be helpful in cataloguing the document. They should be selected so that no security classification is required. Identifiers such as equipment model designation, trade name, military project code name, geographic location may also be included. If possible keywords should be selected from a published thesaurus. e.g. Thesaurus of Engineering and Scientific Terms (TEST) and that thesaurus-identified. If it is not possible to select indexing terms which are Unclassified, the classification of each should be indicated as with the title.)

SAR, Moving Target, Range-Doppler, Velocity Extraction

Defence R&D Canada

Canada's leader in Defence
and National Security
Science and Technology

R & D pour la défense Canada

Chef de file au Canada en matière
de science et de technologie pour
la défense et la sécurité nationale

DEFENCE **R&D** DÉFENSE